



Centre Oceanogràfic
de Balears (COB-IEO)



Spatio-temporal fishing risk of large pelagic fish in the Mediterranean Sea

Master Thesis

Tom Leven

02312706

At the Faculty of Sciences

Ghent University

Main supervisor: Dr. Pilar Tugores

Co-supervisors: Dr. Diego Alvarez-Berastegui & Dr. Miguel Cabanellas-Reboreda

Executive Summary

The executive summary goes here.

Abstract

Abstract goes here.

Contents

Executive Summary	i
Abstract	ii
1 Introduction	1
2 Material and Methods	3
2.1 Data sources	3
2.1.1 Fishing hours	3
2.1.2 ICCAT catch data	4
2.1.3 Bluefin Tuna vessels	5
2.2 Data filtering	5
2.3 Data analysis	7
3 Results	11
3.1 Cumulative apparent fishing hours	11
3.2 Hotspot analysis	12
3.3 Temporal changes	15
3.4 Flag countries	18
3.5 Depth and distance to port	20
4 Discussion	22
5 Conclusion	23
6 Acknowledgements	24
A Supplementary Material	29

1 Introduction

- Delineating fishing grounds essential for fisheries management
- Traditional tools and shortcomings, logbooks, VMS (resolution, ping rate etc.)
- AIS as promising tool to understand fisheries dynamics for example to estimate fishing effort or to aid in fisheries governance (MCS)
 - Explain how AIS works
- Limitations of AIS
- Conservation issues in Mediterranean, highly migratory species
 - New approach in ICCAT to go towards climate informed fisheries
 - TunaMed Observatory
 - Monitor changes in spatio-temporal distribution essential
 - Develop indicators for habitat changes due to climate change but also indicators for human pressures like fishing
- BFT collapse and exploitation history, tuna farms
- Countries report coarse spatial data to ICCAT, if any
- AIS allows fine-scale analysis of spatio-temporal changes
- Metiers for each species, when they are fished, how they migrate
- Research questions:
 - Where and when is fishing activity for large pelagic species most intense and has this changed over time from 2015-2024?

- What are the seasonal patterns of fishing activity by gear type and do they differ interannually?
- To what extent does AIS capture the full scope of fishing activity in the Mediterranean?
- What is the spatial relationship between fishing hours and environmental features such as distance to port, and bathymetry and how does this differ between the two gear types?
- How: Fishing hours data from GFW etc.

2 Material and Methods

2.1 Data sources

2.1.1 Fishing hours

Data on fishing hours was obtained from Global Fishing Watch (GFW). This non-profit organization provides a global dataset of estimated fishing activity derived from AIS data (Global Fishing Watch, 2025). They process data from over 190,000 unique AIS transmitters, each assigned a unique Maritime Mobile Service Identity (MMSI). These AIS devices broadcast a vessel's location as frequently as every 2 seconds (Kontas, n.d.; Taconet et al., 2019). Along with the exact location, each AIS transmission includes a timestamp, speed, and heading of the vessel. GFW then analyses these positional data points via two different Convolutional Neural Networks (CNN's), which are described in detail in Kroodsma et al. (2018), to infer fishing activity.

A first CNN classifies fishing vessels into one of sixteen categories (Fig. 1) and predicts vessel characteristics such as length, tonnage, and engine power. This deep-learning model is trained on a dataset of vessels matched to official vessel registries which are *known* fishing vessels. Vessels without gear information in the registries used are assigned a gear if their movement patterns resemble those of a known vessel class. A second CNN classifies every obtained AIS position as either fishing or non-fishing based on characteristic fishing movement (Kroodsma et al., 2018). These individual fishing events are then aggregated into grid cells spanning either 0.1° or 0.01° on a side. For the present analysis, 0.1° resolution was chosen as the study area includes the whole Mediterranean and is thus, quite large. See Figure 2 for an overview of the GFW processing pipeline.

Unique vessels are identified based on their MMSI number and the dataset con-

tains information on the vessel's registration and flag country. The gear class estimated by the CNN is also compared with the information from different vessel registries, such as the EU fleet register or the ICCAT record of vessels. In case the derived vessel class does not match to the one in the registry, GFW assigns the broadest gear type that allows for agreement. If for example, a vessel is registered as a purse seiner but is inferred to be a tuna purse seiner, it would ultimately be assigned to the purse seiner class (Fig. 1).

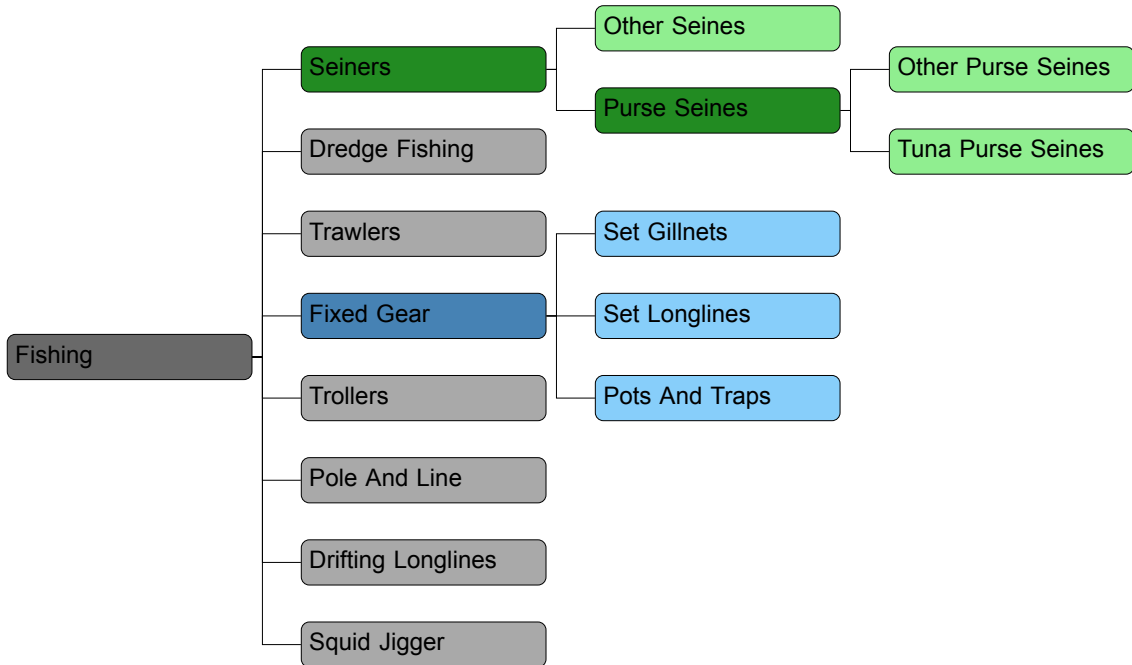


Figure 1: Hierarchy of fishing gears recognised by GFW

2.1.2 ICCAT catch data

Data on catches of large-pelagic species in the Mediterranean is openly available from the International Commission for the Conservation of Atlantic Tunas (ICCAT). Nominal catch data was obtained for the period 2015-2023 and filtered for the major large pelagic species like tunas and billfishes (ICCAT, 2025).

2.1.3 Bluefin Tuna vessels

Individual purse seine vessels that were assigned a bluefin tuna quota for 2024 were obtained from the corresponding national notices. In France, quotas are allocated and published by the *Ministère de la Transition écologique et de la Cohésion des territoires* (2024). In Spain, by the *Secretaría General de Pesca* (2024) and in Italy by the *Ministero dell'agricoltura, della sovranità alimentare e delle foreste* (2024). These countries were chosen exemplary because in the period from 2015 to 2023, they made up more than half of the total landings of BFT for all contracting parties to ICCAT, of which close to 90% are fished with purse seine nets (ICCAT, 2024b). Since the national notices did not contain the vessels MMSI number (which is the identifier used by GFW), the vessel names and registration numbers were cross-referenced with the European Fleet Register to obtain it (European Commission, Directorate-General for Maritime Affairs and Fisheries, 2025).

2.2 Data filtering

All data filtering was conducted using R (v4.4.1; R Core Team, 2024) within the RStudio environment (Posit team, 2024). The GFW dataset was first cropped and adjusted to a shapefile of the Mediterranean Sea, obtained from the General Fisheries Commission for the Mediterranean (GFCM). Subsequent filtering was based on the assigned gear type and GFW registry information. Only entries with the gear type drifting longlines or tuna purse seines, and that were registered with ICCAT were retained (Fig. 2). These gear types were chosen as they are the main *metiers* involved in the exploitation of large-pelagic species in the Mediterranean. Since 2015, on average, 95% of BFT's, and 99% of albacore tunas are caught using either longlines or purse seine nets and close to 100% of swordfish catches use longlines (ICCAT, 2024b,a,c) The GFW dataset is available from the

year 2012 until 2024. However, only entries from 2015 were retained, in order to avoid masking *real* fishing dynamics with the increase in adoption of AIS devices, which only became mandatory in the EU in 2014 for all vessels > 15 m in length (European Commission, 2011). It is estimated however, that in the Mediterranean the EU fishing fleet >15 m is 100% equipped with AIS since 2018 (Taconet et al., 2019).

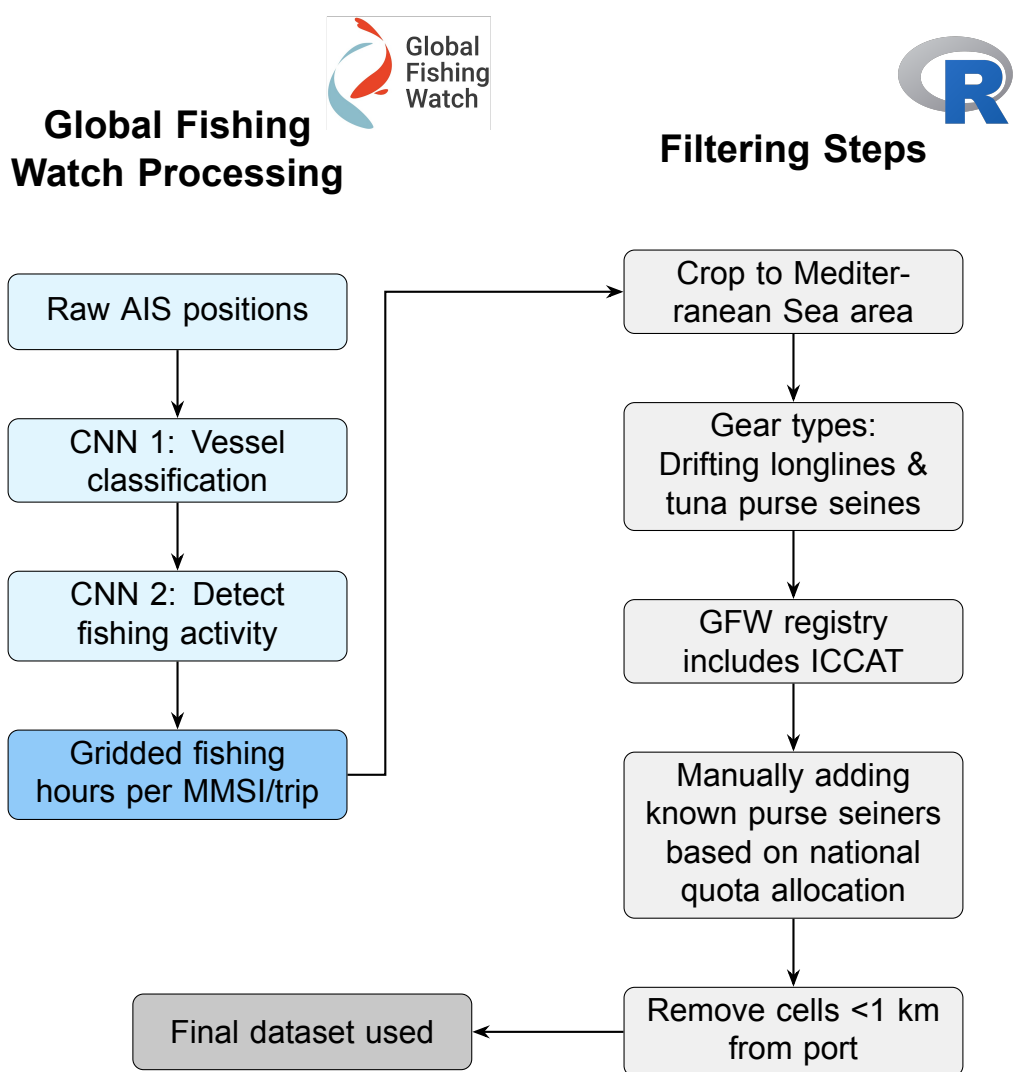


Figure 2: Global Fishing Watch data processing pipeline and filtering steps to obtain the final dataset used in this study. CNN = Convolutional Neural Network

In case of the tuna purse seiners, these filtering steps also removed some vessels

which are known to be fishing for bluefin tuna based on national quota allocations (obtained for Spain, France, and Italy). These vessels were removed by the filtering steps either because GFW assigns them a different gear type, or they are not present in the registry information from ICCAT that GFW uses. For the present analysis, these vessels were thus, manually included from the curated list of tuna purse seiners based on the national vessel registries.

Irregular vessel movement patterns occurring in or near ports can falsely resemble fishing activity and should therefore be excluded when estimating fishing effort. These movements include cruising towards the harbour to land catches or vessel maintenance (de Souza et al., 2016). Thus, to remove these areas from the analysis, the points inside the 1 km boundary around ports were removed. Distance from port was determined based on a dataset from GFW, which contains anchorages that are either known ports, or that contained at least 20 unique stationary vessels since 2012 (Global Fishing Watch, 2020).

2.3 Data analysis

To identify persistent hotspot areas throughout the one decade study time and analyse spatio-temporal trends, the *Emerging Hotspot Analysis* (EHA) tool was used in ArcGIS Pro (Esri Inc., 2024). For this, multidimensional netCDF (network common data form) files of the fishing hours data were generated after curation and filtering in R, using the ‘terra’ package (v1.8.18; Hijmans, 2025). Subsequently, they were read in as multidimensional raster files in ArcGIS Pro, with the dimensions corresponding to longitude, latitude and time. Data was aggregated annually, using the sum of fishing hours per year for each cell. From this, I created a space-time cube which is the input required for the EHA tool (Fig.3).

EHA uses a combination of two statistical methods. First, the Getis-Ord G_i^* statistic to identify areas where low/high values are spatially clustered (Getis and Ord,

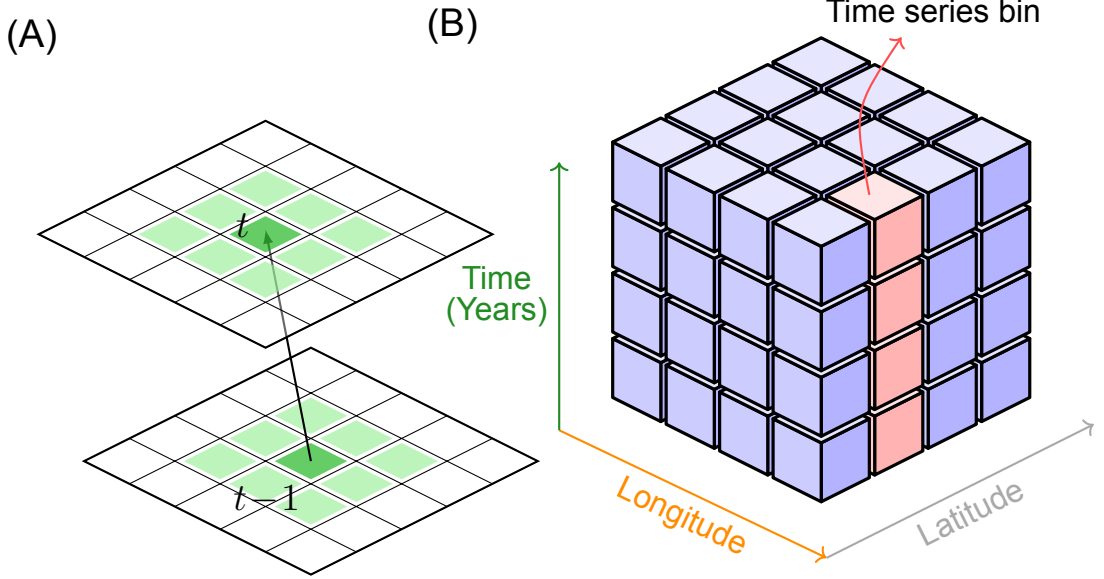


Figure 3: A) Conceptualization of space-time dependency as implemented in the Emerging Hotspot Analysis tool. One *neighbourhood bin* is defined as the cell itself (darkgreen) plus the cells surrounding it (lightgreen), as well as those cells in the previous time step. B) Structure of the space-time cube in ArcGIS. Each individual cube corresponds to one *neighbourhood bin*. One *time series bin* corresponds to the same location over time (red).

1992). The null hypothesis states that the sum of values of location i and its neighbours, is not significantly different from what would be expected by chance, based on all observations. In our case, neighbours are defined as shown in Figure 3A. So each *neighbourhood* contains the cell itself, plus all cells contiguous with it via edges and corners at time t and $t - 1$. Each neighbourhood is compared to all global observations at the current and preceding time step. Based on the neighbourhood definition, a binary spatial weight matrix is constructed, where each entry $w_{i,j}$, is either 1 (if features i and j are neighbours) or 0 otherwise. The G_i^* statistic is then calculated as:

$$G_i^* = \frac{\sum_{j=1}^n w_{i,j} x_j - \bar{X} \sum_{j=1}^n w_{i,j}}{S \sqrt{\frac{n \sum_{j=1}^n w_{i,j}^2 - \left(\sum_{j=1}^n w_{i,j} \right)^2}{n-1}}} \quad (1)$$

where x_j is the value for feature j , $w_{i,j}$ is the spatial weight between feature i and j , and n is the total number of features. The terms \bar{X} and S represent the global mean and standard deviation of the attribute values, respectively, and are given by:

$$\bar{X} = \frac{\sum_{j=1}^n x_j}{n} \quad (2)$$

$$S = \sqrt{\sqrt{\frac{\sum_{j=1}^n x_j^2}{n}} - (\bar{X})^2} \quad (3)$$

The implementation of G_i^* in the EHA tool also applies a False Discovery Rate (FDR) correction to account for multiple testing and spatial dependency in the data. This approach is preferred over methods like Bonferroni correction, which only accounts for multiple testing, as FDR is less conservative and less likely to miss true positives (Caldas de Castro and Singer, 2006). EHA is thus, a spatio-temporal extension of the G_i^* statistic, as it extends each cell not only to its spatial but also to the temporal neighbours.

Second, EHA applies the Mann-Kendall trend test to evaluate whether there is a monotonic upward or downward trend in each time series bin (Mann, 1945; Kendall and Gibbons, 1990). The non-parametric Mann-Kendall statistic S analyses each time series bin. It ranks and compares each point x_i (for $i = 1, 2, \dots, n - 1$) to all subsequent points x_j (for $j = i + 1, i + 2, \dots, n$) and is given by (Kendall and Gibbons, 1990, Section 1.9)

$$S = \sum_{i=1}^{n-1} \sum_{j=i+1}^n \text{sign}(x_j - x_i) \quad (4)$$

Where the sign function is defined as:

$$\text{sign}(x_j - x_i) = \text{sign}(R_j - R_i) \begin{cases} 1 & x_i < x_j \\ 0 & x_i = x_j \\ -1 & x_i > x_j \end{cases} \quad (5)$$

and R_i and R_j are the ranks of observations x_i and x_j of each time series. Thus, for every time point, it assigns a 1 if the value is higher than the previous one, a 0 if the value is the same, and a -1 if the value is lower. These scores are then summed for each time series bin and under the null hypothesis of no trend, the value of S is zero. To assess the significance of S , the variance V_0^* can be calculated as (Kendall and Gibbons, 1990, Section 5.6)

$$V_0^*(S) = n(n-1)(2n+5)/18 - \sum_{j=1}^m t_j(t_j-1)(2t_j+5)/18 \quad (6)$$

where n is the total number of observations, and m the number of groups with tied ranks, each with t_j tied observations.

3 Results

3.1 Cumulative apparent fishing hours

In total, there were 213 unique longliners and purse seiners recorded for 2015–2024. These vessels together accounted for an average of 5115 fishing days per year, with an average of 24 days per vessel per year.

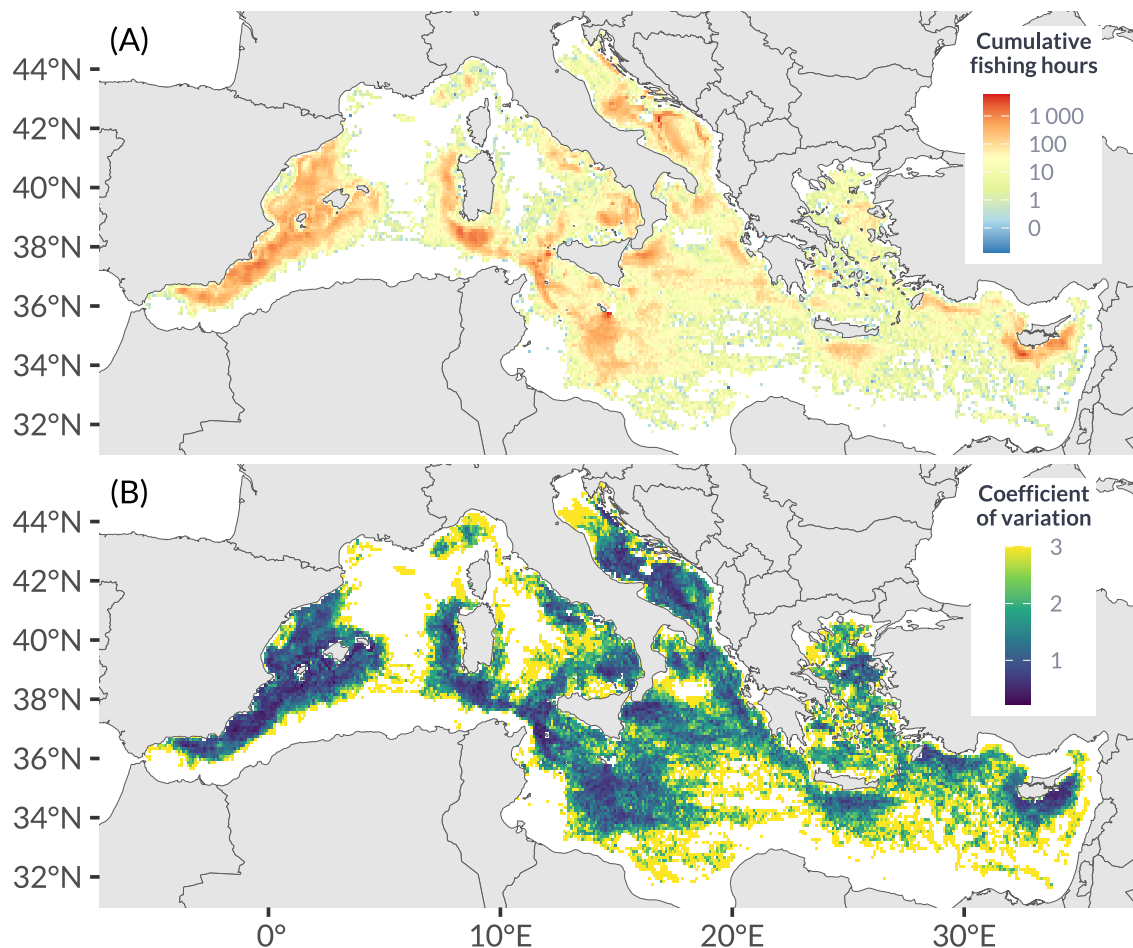


Figure 4: Summary statistics for both longliners and purse-seiners. A) Cumulative fishing hours in the Mediterranean (2015–2024). Colors are on a log-scale. B) Coefficient of variation between years (standard deviation divided by mean) for each cell.

Areas that show the highest effort throughout the study time include the Mediterranean coast of Spain, around Sardinia and Sicily, south of Malta, the Adriatic, and south of Cyprus (Fig. 4A). Areas with high effort generally also show the lowest

coefficient of variation (Fig. 4B). There does not appear to be any fishing activity based on AIS around the African Mediterranean coast.

3.2 Hotspot analysis

There were numerous persistent longline hotspot areas identified throughout the Mediterranean including the southern coast of Spain, south of Sardinia, around Sicily and Malta, as well as south of Cyprus (Fig. 5A). These hotspots show however, differing trends. Fishing hours in the south of Malta appear to be increasing throughout, with a similar trend of increase in the Adriatic Sea. Other areas that appear to be consistent hotspots like the east of Sicily show a decreasing trend (Fig. 5B).

Purse seine hotspots appear persistent around the Balearic Islands, in the Adriatic Sea, and along the Calabrian coast in Italy (Fig. 6A). Trends in these areas show a clear increase around Ibiza and in the central Adriatic while areas around the coast in the Adriatic show a decrease (Fig. 6B). The hotspot area along Calabria shows no clear trend.

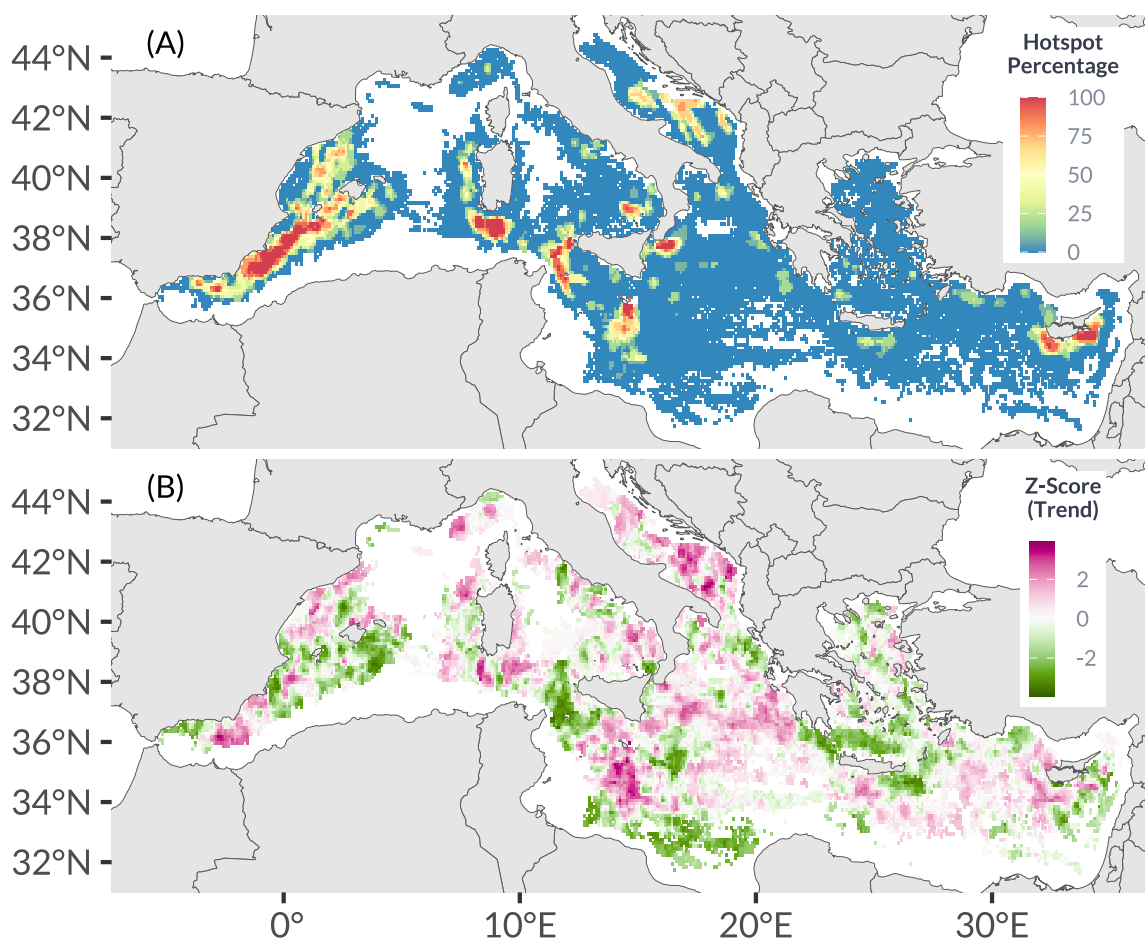


Figure 5: Hotspot percentage and trend scores for longliners in the Mediterranean. The percentage reflects the years in which a given cell was a hotspot based on the Getis-Ord G_i^* statistic. The Z-score is derived from the Mann-Kendall statistic.

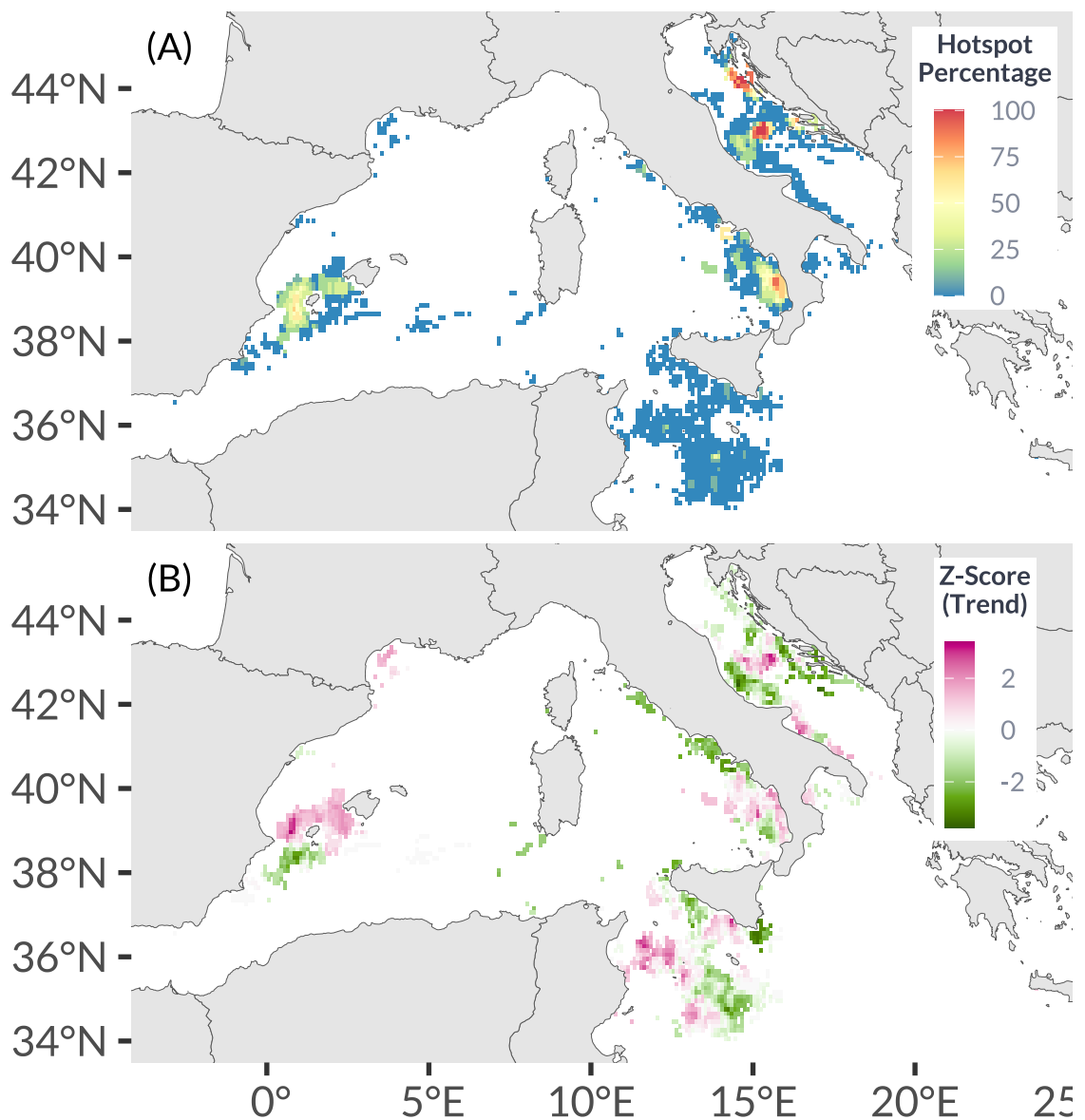


Figure 6: Hotspot percentage and trend scores for purse seiners in the Mediterranean. The percentage reflects the years in which a given cell was a hotspot based on the Getis-Ord G_i^* statistic. The Z-score is derived from the Mann-Kendall statistic.

3.3 Temporal changes

Longline fishing hours show a clear seasonal trend where activity is highest in the summer and lowest in the winter (Fig. 7A). Some areas show high effort earlier in the season in spring (for example south of Malta) and others are more persistent later in the season in fall (for instance around Ibiza). Daily fishing shows a similar seasonal trend, although the intensity varies between years. The highest annual longline fishing hours throughout the study time were recorded for 2022 and the lowest for 2015 (Tab. 1).

Table 1: Annual sum of fishing hours for purse seiners and longliners.

Year	Fishing hours	
	Purse seiners	Longliners
2015	4,193	71,846
2016	5,313	89,136
2017	5,901	107,345
2018	6,128	106,130
2019	5,931	113,261
2020	5,636	124,927
2021	5,706	133,361
2022	5,675	149,059
2023	5,085	139,068
2024	6,661	137,406

Purse seine fishing hours show a very pronounced seasonal trend with a peak in spring (Fig. 8). The core areas of the fishery during spring are the Balearic Islands, along the coast of Calabria (south-west Italy), and the central Adriatic. In the Adriatic, there appears to be purse seine activity throughout the whole year (Fig. 8A). The purse seine season for large-pelagic species is limited to the months of May and June and is consistent between years (Fig. 8B). Highest annual fishing hours for purse seiners were recorded in 2024 and the lowest in 2015 (Tab. 1).

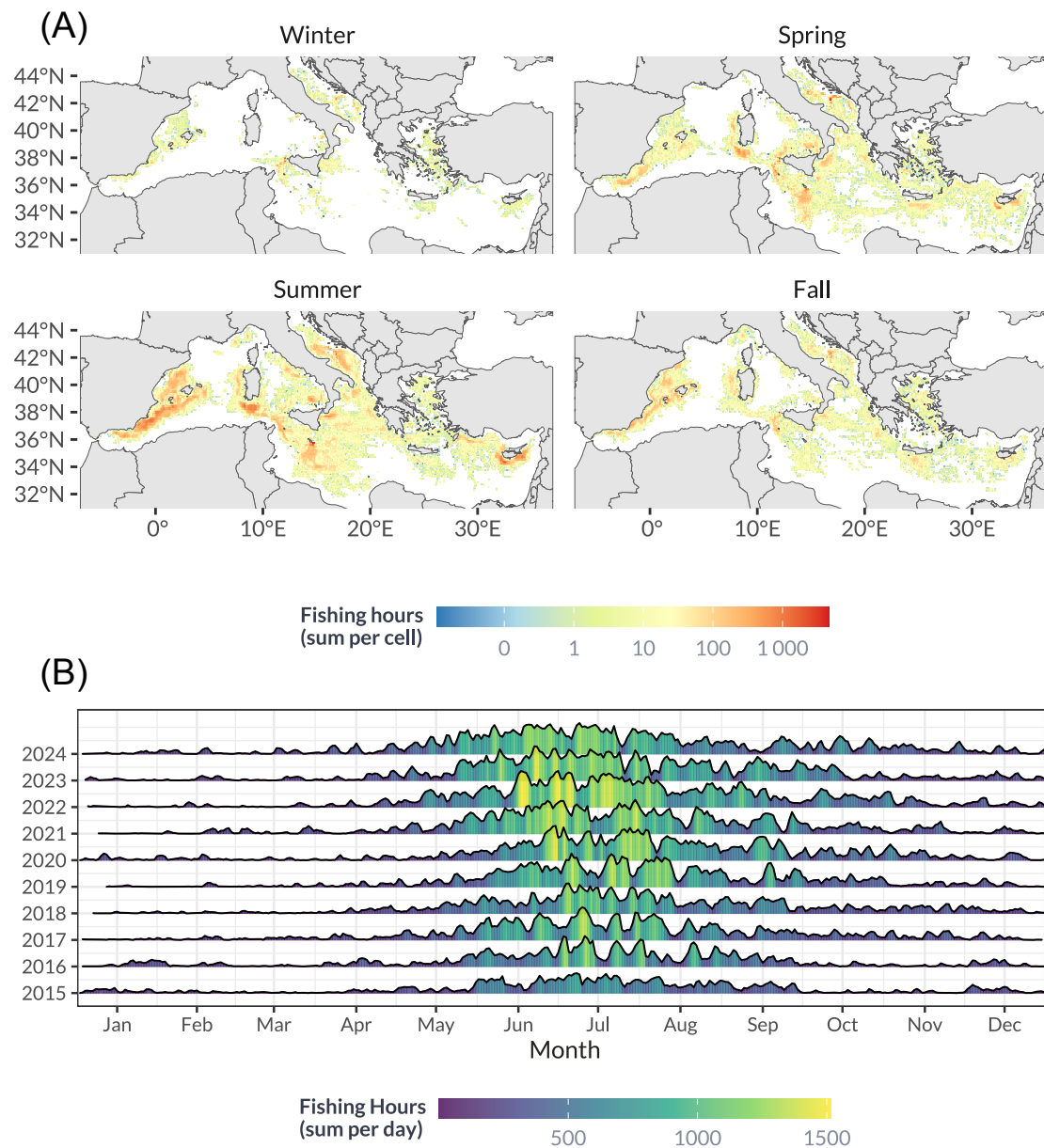


Figure 7: Temporal changes in longline fishing hours. A) Spatial differences between seasons. Hours are summed per season and cell. B) Time series of fishing hours, summed per year and day.

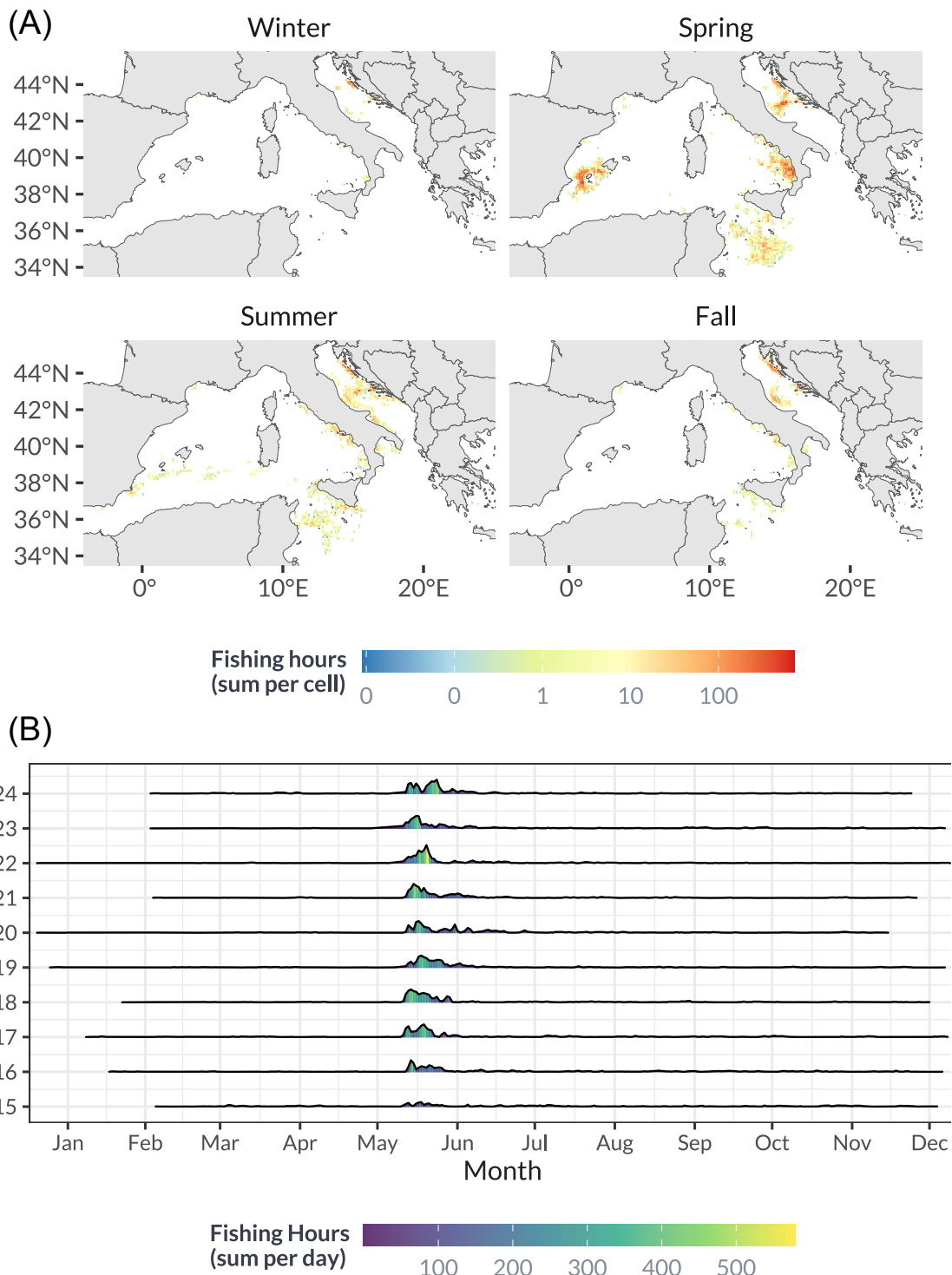


Figure 8: Temporal changes in purse seine fishing hours. A) Spatial differences between seasons. Hours are summed per season and cell. B) Time series of fishing hours, summed per year and day.

3.4 Flag countries

Vessels were flagged to a total of 10 countries and the majority of vessels analysed were longliners (Tab. 2). For an overview of fishing hours for each country see Figure S1 and S2. Italy has the highest amount of both purse seiners and longliners in the GFW data.

Table 2: Number of vessels by country and gear type based on GFW data and national registry information. ‘–’ indicates no recorded vessels for that gear.

Country	Number of vessels	
	Purse seiners	Longliners
Algeria	4	–
Croatia	2	–
Cyprus	–	25
France	14	–
Greece	–	9
Italy	16	79
Malta	–	21
Morocco	1	–
Spain	5	35
Tunisia	2	–
Total	44	169

Most regions with high fishing activity also have vessels flagged to multiple countries fishing in the same area. Regions with high overlap between flag countries for longliners include the Balearic Islands, south of Crete, and south of Malta (Fig. 9), which are also areas with high fishing hours (Fig. 4A). For purse seiners, fishing generally is more concentrated and thus, overlap is also higher, as seen in the core fishing areas of the Balearic Islands and south of Malta (Fig. 9).

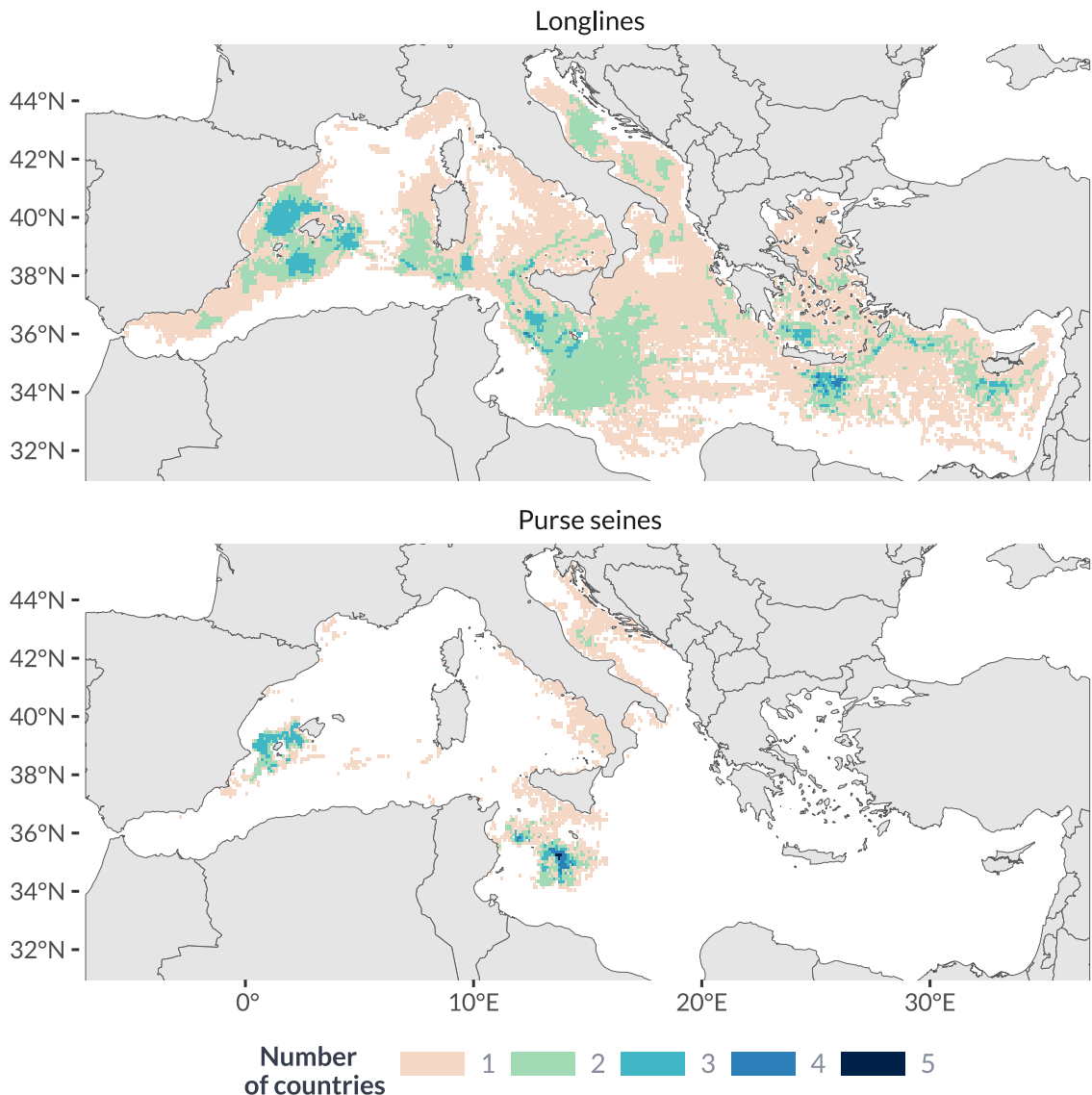


Figure 9: Number of countries fishing per cell for longliners and purse seiners between 2015-2024.

A comparison of fishing hours from the GFW data with catch data from ICCAT shows that AIS underrepresents fishing activity by non-EU countries relative to EU countries (Fig. 10). Even though, many non-EU countries account for a substantial share of the total reported catches. Notably, AIS also does not capture any French longline vessels.

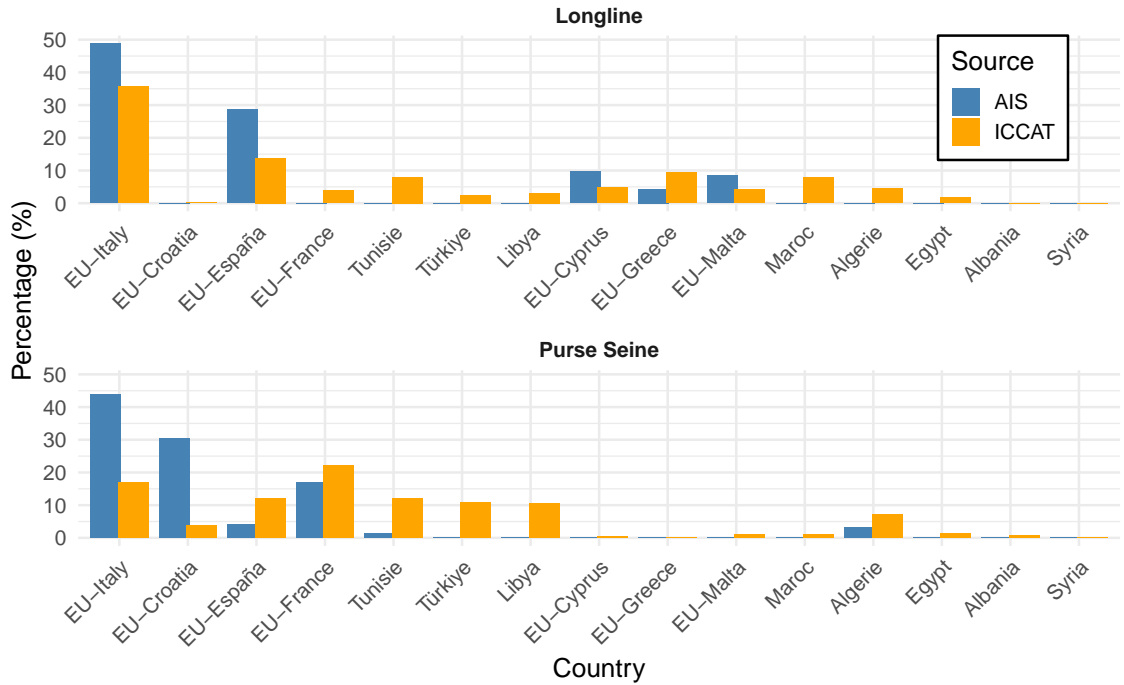


Figure 10: Comparison of relative percentages between GFW AIS data and IC-CAT catch data. AIS percentages are relative to the total fishing hours between all countries. ICCAT percentages are relative to the total weight of catches between all countries.

3.5 Depth and distance to port

The relationship between the cumulative proportion of fishing hours and the distance to port reveals that most fishing activity of both gear types is concentrated less than 100 km from the closest port (Fig. 11A). The trend for the depth is different between gear types, where most purse seine fishing occurs at shallower depths (below 1000 m) and longline effort takes place over much greater depth ranges (Fig. 11B).

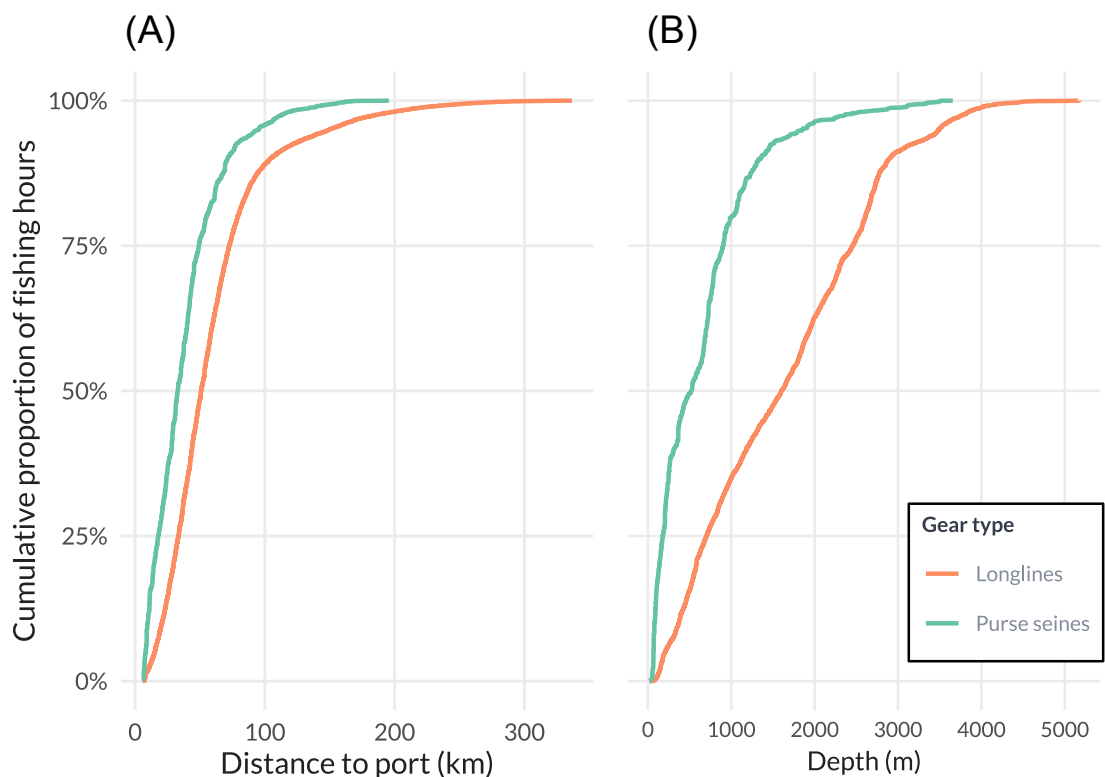


Figure 11: Cumulative proportion of fishing hours with A) Distance to port and B) Depth.

4 Discussion

- Summarize findings and methods
- Compare with other studies looking into effort of these gear types
 - Not possible to get effort per metier with AIS (at least with GFW methods right now) -> problematic
- Shortcomings of AIS
 - What are the caveats identified during the study?
 - Which different methods exist to analyse AIS data? Which one is suitable when and for what?
- What can we infer from AIS derived fishing activity and what not?
- Future perspectives

5 Conclusion

Conclusion goes here.

6 Acknowledgements

Thank you to...

Bibliography

Marcia Caldas de Castro and Burton H. Singer. Controlling the false discovery rate: A new application to account for multiple and dependent tests in local statistics of spatial association. *Geographical Analysis*, 38(2):180–208, 2006. URL <https://onlinelibrary.wiley.com/doi/abs/10.1111/j.0016-7363.2006.00682.x>.

Erico N. de Souza, Kristina Boerder, Stan Matwin, and Boris Worm. Improving fishing pattern detection from satellite ais using data mining and machine learning. *PLOS ONE*, 11(7):1–20, 07 2016. URL <https://doi.org/10.1371/journal.pone.0158248>.

Esri Inc. ArcGIS Pro (Version 3.4). <https://www.esri.com/en-us/arcgis/products/arcgis-pro/overview>, 2024. Esri Inc.

European Commission. Commission Directive 2011/15/EU of 23 February 2011 amending Directive 2002/59/EC of the European Parliament and of the Council establishing a Community vessel traffic monitoring and information system Text with EEA relevance. *Official Journal of the European Union*, L49/33, 2011. URL <https://eur-lex.europa.eu/legal-content/EN/TXT/PDF/?uri=CELEX:32011L0015>.

European Commission, Directorate-General for Maritime Affairs and Fisheries. Eu fleet register, version 1.2.0.1, 2025. URL https://webgate.ec.europa.eu/fleet-europa/index_en. Accessed 2025-05-17.

Arthur Getis and J. K. Ord. The analysis of spatial association by use of distance statistics. *Geographical Analysis*, 24(3):189–206, 1992. URL <https://onlinelibrary.wiley.com/doi/abs/10.1111/j.1538-4632.1992.tb00261.x>.

Global Fishing Watch. Distance from port in meters, Version 20201104,

2020. URL <https://globalfishingwatch.org/data-download/datasets/public-distance-from-port-v1>.

Global Fishing Watch. Global AIS-based Apparent Fishing Effort Dataset, Version 3.0, 2025. URL <https://doi.org/10.5281/zenodo.14982712>.

Robert J. Hijmans. *terra: Spatial Data Analysis*, 2025. URL <https://rspatial.org/>. R package version 1.8-18, <https://rspatial.github.io/terra/>.

ICCAT. Executive Summary ALB-MD, 2024a. URL https://www.iccat.int/Documents/SCRS/ExecSum/ALB_MED_ENG.pdf.

ICCAT. Executive Summary BFT-E, 2024b. URL https://www.iccat.int/Documents/SCRS/ExecSum/BFT_E_ENG.pdf.

ICCAT. Executive Summary SWO-MD, 2024c. URL https://www.iccat.int/Documents/SCRS/ExecSum/BFT_E_ENG.pdf.

ICCAT. Nominal catches of Atlantic tunas and tuna-like fish (including sharks), by gear, region and flag (Excel table), 2025. URL https://www.iccat.int/Data/t1nc_20250131.7z.

M. G. Kendall and J. D. Gibbons. *Rank Correlation Methods*. Griffin, London, 5th edition, 1990.

Vasilis Kontas. How often do the positions of the vessels get updated on Marine Traffic?, n.d. URL <https://support.marinetraffic.com/en/articles/9552905-how-often-do-the-positions-of-the-vessels-get-updated-on-marinetraffic>. Retrieved 5 January 2025.

David A. Kroodsma, Juan Mayorga, Timothy Hochberg, Nathan A. Miller, Kristina Boerder, Francesco Ferretti, Alex Wilson, Bjorn Bergman, Timothy D. White, Barbara A. Block, Paul Woods, Brian Sullivan, Christopher Costello, and Boris Worm. Tracking the global footprint of fisheries. *Science*, 359(6378):904–908,

2018. doi: 10.1126/science.aa05646. URL <https://www.science.org/doi/abs/10.1126/science.aa05646>.

H. B. Mann. Nonparametric tests against trend. *Econometrica*, 13:245–259, 1945.

Ministero dell'agricoltura, della sovranità alimentare e delle foreste. Allegato 1, TONNO ROSSO - CAMPAGNIA DI PESCA 2024. *Gazzetta Ufficiale della Repubblica Italiana*, (117), 2024. URL https://www.gazzettaufficiale.it/atto/serie_generale/caricaDettaglioAtto/originario?atto.dataPubblicazioneGazzetta=2024-05-21&atto.codiceRedazionale=24A02500&elenco30giorni=false.

Ministère de la Transition écologique et de la Cohésion des territoires. Arrêté du 13 février 2024 établissant les modalités de répartition du quota de thon rouge (*Thunnus thynnus*) accordé à la France pour la zone «océan Atlantique à l'est de la longitude 45° O et Méditerranée» pour l'année 2024. *Journal officiel de la République française*, (Texte 20 sur 103), 2024. URL https://www.legifrance.gouv.fr/download/pdf?id=wSCtx11Gzpq9uWOcYXc7s-_AvWkqbw3aGTWSBldcbDg=.

Posit team. *RStudio: Integrated Development Environment for R*. Posit Software, PBC, Boston, MA, 2024. URL <http://www.posit.co/>.

R Core Team. *R: A Language and Environment for Statistical Computing*. R Foundation for Statistical Computing, Vienna, Austria, 2024. URL <https://www.R-project.org/>.

Secretaría General de Pesca. Resolución de 8 de marzo de 2024, de la secretaría general de pesca, por la que se dispone la asignación de cuotas de atún rojo y publicación del censo específico de la flota autorizada para el ejercicio de la pesca del atún rojo creado por el real decreto 46/2019, de 8 de febrero, por el que se regula la pesquería de atún rojo en el atlántico oriental y mediterráneo.

Boletín Oficial del Estado, (70):32846–32871, 2024. URL <https://www.boe.es/boe/dias/2024/03/20/pdfs/BOE-A-2024-5591.pdf>.

M. Taconet, D. Kroodsma, J. Gee, and J. A. Fernandes. Introduction of Global Atlas of AIS-based fishing activity. In M. Taconet, D. Kroodsma, and J. A. Fernandes, editors, *Global Atlas of AIS-based fishing activity - Challenges and opportunities*. FAO, Rome, 2019. URL <http://www.fao.org/3/ca7012en/ca7012en.pdf>.

A Supplementary Material

Annex 1

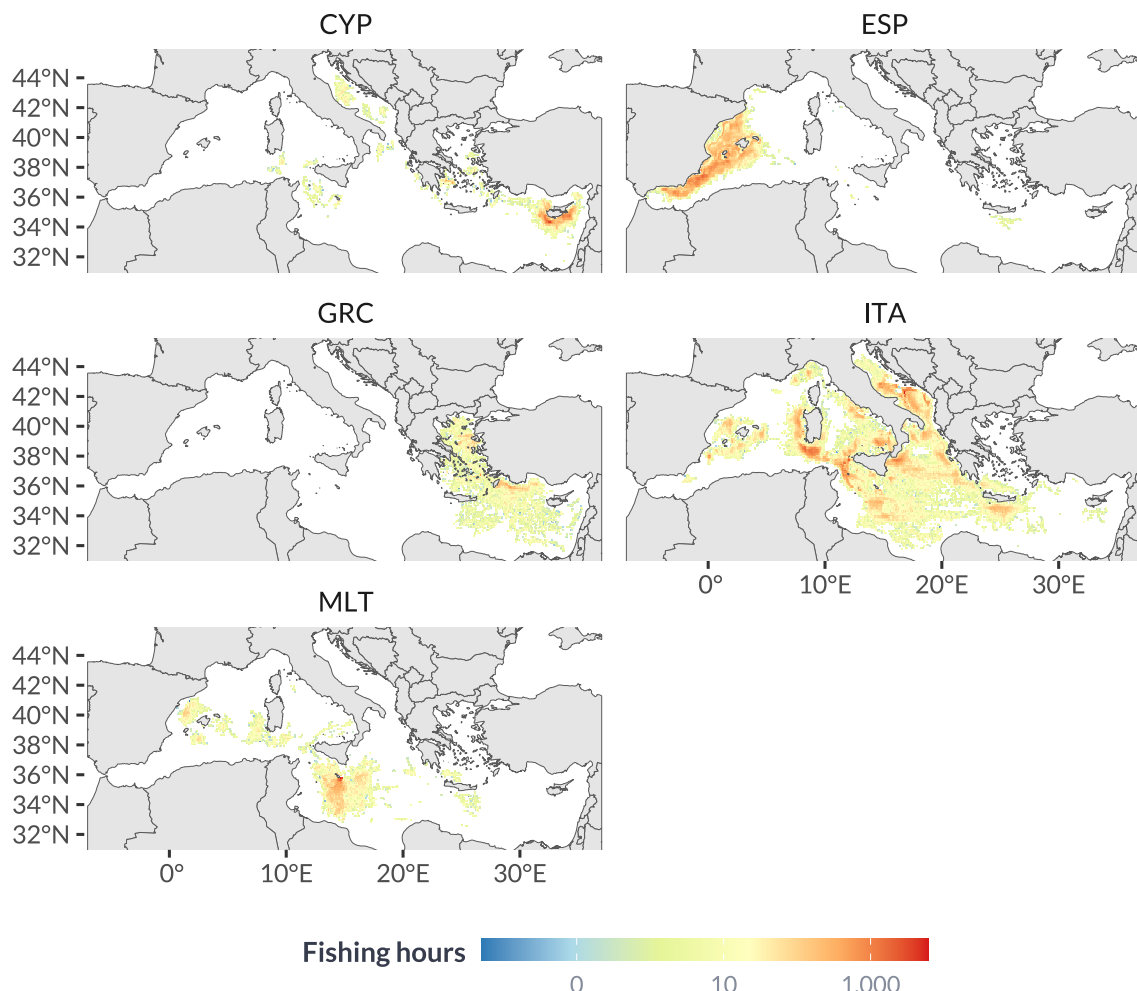


Figure S1: Sum of longline fishing hours per flag country (2015-2024). CYP = Cyprus; ESP = Spain, GRC = Greece, ITA = Italy, MLT = Malta

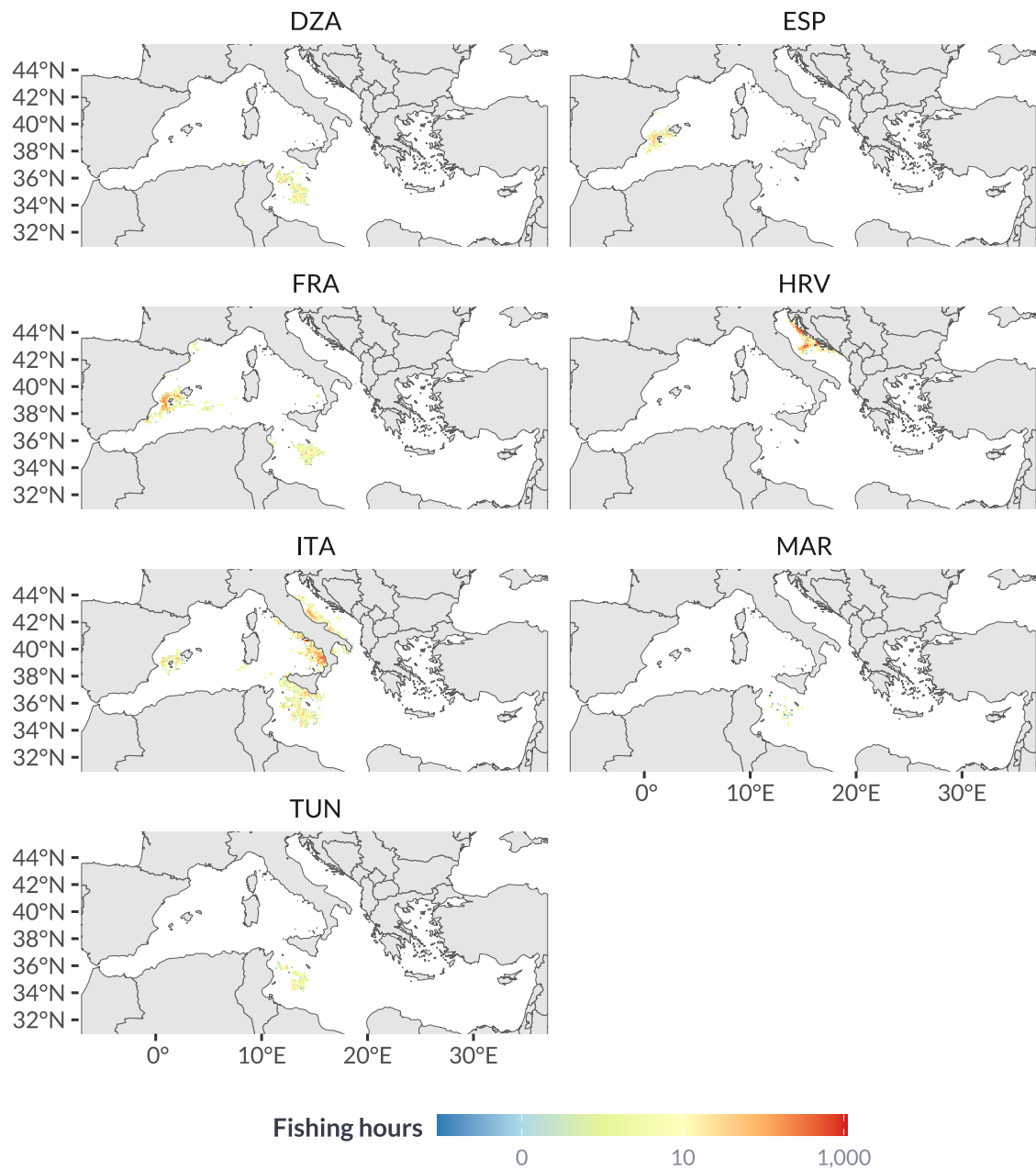


Figure S2: Sum of purse seine fishing hours per flag country (2015-2024). DZA = Algeria, ESP = Spain, FRA = France, HRV = Croatia, ITA = Italy, MAR = Morocco, TUN = Tunisia.